Summer Outdoor Thermal Risk Area Mapping on a University Campus in Auckland, New Zealand

Saghar Hashemi[a], Amirhosein Ghaffarianhoseini[a], *Ali Ghaffarianhoseini[a], Nicola Naismith[a], Sahar Barmomanesh[b], David Sailor[c] & Umberto Berardi[d]

[a] *Department of Built Environment Engineering, School of Future Environments, Faculty of Design and Creative Technologies, Auckland University of Technology, Auckland, New Zealand*

[b] *School of Engineering, Computer and Mathematical Sciences, Faculty of Design and Creative Technologies, Auckland University of Technology, Auckland, New Zealand*

[c] *School of Geographical Sciences and Urban Planning, Arizona State University, USA*

[d] *Faculty of Architectural Science, Toronto Metropolitan University, Toronto, Canada*

*: ali.ghaffarianhoseini@aut.ac.nz , WZ1213, WZ Building, AUT City Campus, 6-24 St Paul Street, Auckland Central, Auckland, 1010, New Zealand. Telephone Number: +64 9 921 9999 (Work)

Abstract:

This study aimed to identify thermal risk areas at the city campus of Auckland University of Technology (AUT), New Zealand, and analyze future thermal patterns using Physiologically Equivalent Temperature (PET) simulations for the summers of 2050 and 2080. A multi-layered approach involving hazard, exposure, and vulnerability layers was used. High thermal stress areas were identified based on PET values exceeding 23°C, exposure zones were determined by analyzing usage intensity which means dividing the number of people within a specific zone by the total number of people present in the entire selected location, and vulnerability areas were identified through participant questionnaires. Two locations were investigated and future climate data based on the climate change world weather file generators (CCWorldWeatherGen) and represent concentration pathways (RCPs) namely the RCP8.5 projected increased PET values for both locations. Proposed scenarios for mitigating thermal stress involved introducing greenery. Replacing a concrete wall with a green wall in location one resulted in a 2°C average PET reduction (from 22°C to 20°C), and planting trees in location two led to a 3°C average PET reduction (from 25°C to 22°C). The findings provide valuable insights for urban planners and architects in New Zealand, aiding in the identification of thermal risk areas and the implementation of strategies to enhance outdoor spaces' livability in different urban contexts.

Keywords:

Thermal risk areas; Outdoor thermal comfort; Urban microclimate; PET value; Auckland; Greenery

1.Introduction

Over the past few decades, urbanization has resulted in transformations in the physical structure and form of cities[1]; The complexity of urban areas, characterized by variations in urban densities, layout typologies, and architectural forms, gives rise to intricate microclimate conditions[2, 3].The perception of the outdoor thermal environment by an individual can be influenced by both the outdoor climate and the surrounding built environment[4]. An inadequately designed environment can also impact microclimate conditions, potentially compromising thermal comfort[5]. Therefore, the focus of this study is to investigate environmental designs that assesses outdoor thermal conditions based on current and future climate patterns.

A relatively small number of studies on urban microclimate and outdoor thermal comfort have been conducted in New Zealand[6-11]. In New Zealand, climate change is causing an upward trend in both the average and maximum temperatures[12, 13]. There is a projected substantial rise in the frequency of days where temperatures exceed 25 degrees Celsius[14].There is a notable lack of evidence indicating that future urban development and climate change adaptation plans in New Zealand, particular Auckland take into account the assessment of future urban microclimate, urban heat island (UHI) effects, and outdoor thermal comfort[11]. The scale and intensity of urban development in Auckland, as the largest and most populous city in New Zealand, combined with the anticipated escalation of summer overheating events resulting from anthropogenic climate change, necessitate a comprehensive investigation into the outdoor thermal comfort conditions within the city[11].

Hence, the primary objectives of this study, in line with these concerns, are as follows:

1.To identify outdoor thermal risk areas in the selected locations within of Auckland University of Technology (AUT) based on current microclimate conditions.

2.To predict future thermal conditions of the identified thermal risk areas based on future climate patterns.

3. To assess the impact of the use of greenery on high thermal risk areas.

2. Method

2.1. Research structure

This research consists of two steps. In step one, the two most crowded outdoor areas of AUT are identified, and step two is divided into four different phases.In phase one, we examined outdoor thermal risk areas. The initial phase of the study involved the establishment of three distinct layers: the hazard layer, exposure layer, and vulnerability layer, for the selected locations as recommended by Huang[5]. Each layer was constructed using a combination of field measurements, field observations, and software simulations. By overlaying the layers of hazard, exposure, and vulnerability, areas with high thermal risk were identified[5]. While many previous research[5, 15, 16] did this method, no one has done it for Auckland. To assess the future changes in thermal comfort through simulations in phase two, data from two future time periods were considered. And finally, For phase three, we examined new scenarios to mitigate thermal stress in these areas (Figure 1).

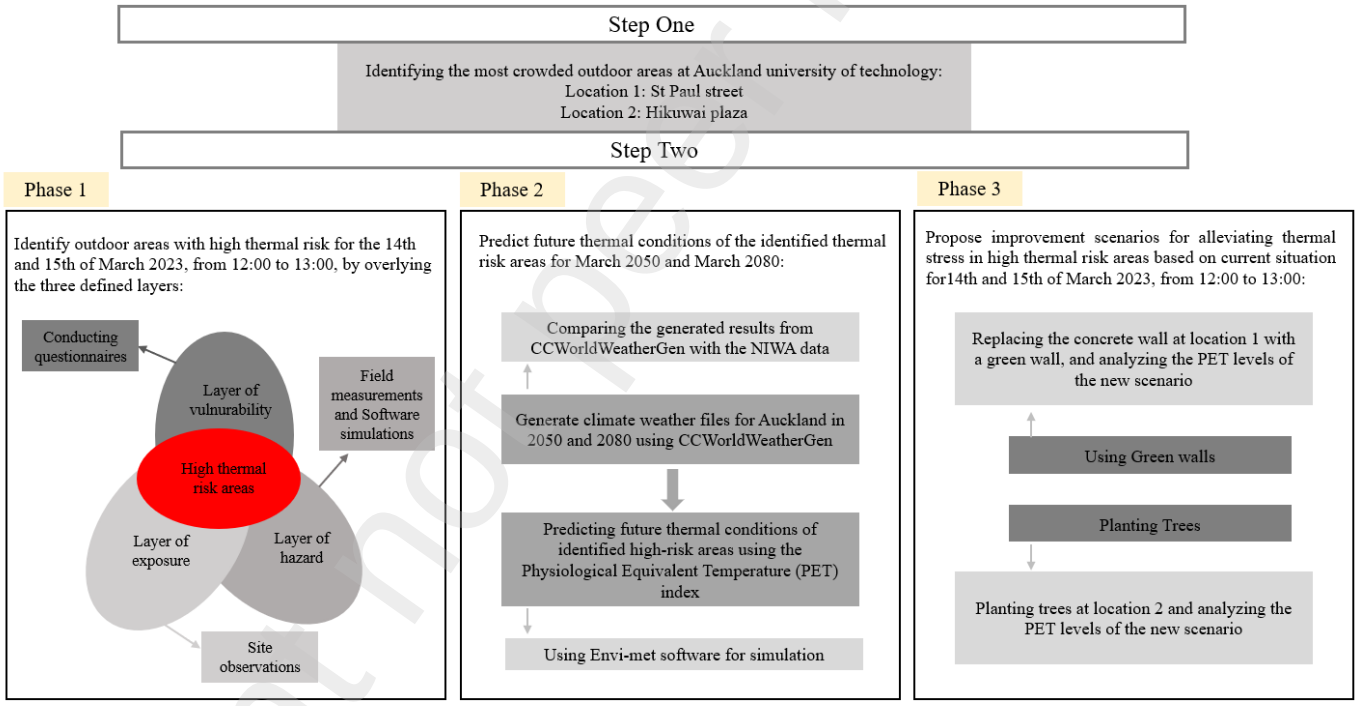

Figure 1. The structure of the research

The research location is the city campus of Auckland University of Technology (S-36° 51', E174° 46'). To identify outdoor thermal risk areas at this university, we selected two highly frequented outdoor places. The first is a street called St Paul, measuring 200*15m, which is surrounded by nine different buildings ranging from 8m to 48m in height. The main materials used for these buildings are glass, concrete, and steel, with a combination of asphalt and concrete pavements. The second location is a plaza called Hikuwai, covering an area of 900m^2, and it is surrounded by three different buildings ranging from 8m to 24m in height. These buildings are constructed using glass, concrete, and steel materials. Both locations have limited vegetation coverage.

In Auckland, the annual average temperature is 15.5°C, with the monthly average reaching 20°C in the hottest month, February, and dropping to 11.5°C in the coldest month, July[17]. For this research, we specifically selected the dates of March 14th and 15th as representative summer days to identify thermal risk areas. The rationale behind choosing this location and timeframe is that universities provide a conducive environment for conducting field surveys and gathering perceptions on outdoor thermal comfort from individuals of diverse ages and nationalities. Furthermore, in New Zealand, March marks the beginning of the semester, and the 14th and 15th of March fall on Tuesday and Wednesday, which are the days when most classes are held at AUT. This allows us to engage with a larger population and identify thermal risk areas during the summer season.

2.2. Defining the layer of hazard (Phase 1a)

In this study, the term "hazard" pertains to the presence of thermal stress in a particular area[5]. To assess the risk associated with thermal stress, the research utilized the Physiological Equivalent Temperature (PET) index. The PET index serves as a metric for evaluating the level of thermal risk present in a specific location[18]. Higher PET values indicate a greater degree of thermal risk within the examined area[5]. Envi-met is employed to model the complete thermal environment, a capability that has been affirmed through numerous research endeavours demonstrating its efficacy in replicating neighbourhood-scale thermal conditions. [19, 20]. Envi-met is a three-dimensional microclimatic model with a one-dimensional boundary model, three-dimensional atmospheric model, soil model, and plant model[21, 22]. The study grid measures 2 m x 2 m x 2 m and is based on a model with a grid size of 200 x 100 x 60 and 220 x 180 x 40.

The validity of the simulated data was assessed by comparing observed and simulated meteorological data values. We conducted field measurements, using the Davis 6152 Wireless Vantage Pro2 weather station (Figure2). The Vantage Pro2 uses high-quality sensors that are designed to provide accurate and reliable measurements of temperature, humidity, wind speed, direction, and rainfall. The sensors used in the Vantage Pro2 are accurate to within ±0.5 °C for temperature, ±2% for relative humidity, ±2.2 km/h for wind speed, and ±5% for rainfall. Two locations on St Paul Street and Hikuwai Plaza were selected for field measurements based on their potential to provide diverse degrees of shade. The sensors were placed at pedestrian level with a height of 1.5 meters during the measurement process. The meteorological conditions at these locations were constantly monitored and recorded every 30 minutes from 8:30 to 16:30 on March 14, and March 15, 2023.

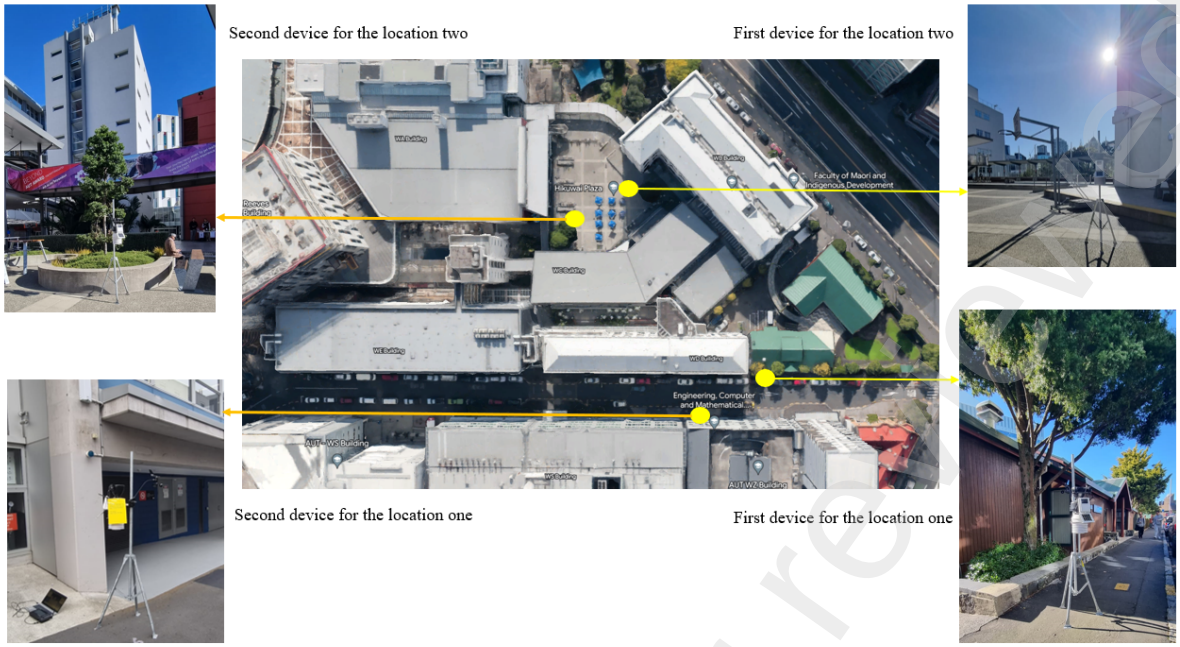

Figure 2. The locations of Davis 6152 Wireless Vantage Pro2 weather stations

2.3. Defining the layer of exposure (Phase 1b)

In this study, exposure is defined as the spatial intensity distribution of individuals using the outdoor space[5]. The level of exposure is determined by the concentration of people gathered in a particular area. Higher exposure is observed in areas with a larger number of individuals present. This data was utilized to calculate the usage intensity of the area, providing insight into the degree of exposure experienced by the space users[5]. The construction of the exposure layer involves a stepwise process. Firstly, the locations were divided into zones. In this study, we divided two specific locations into zones based on the arrangement of sitting facilities and shading conditions. St Paul Street (location one) was divided into three zones, while Hikuwai Plaza (location two) was divided into five zones. Secondly, the number of individuals within each zone was hand-counted specifically from 12:00 to 13:00 on March 14th, 2023, for location one, and on March 15th, 2023, for location two by researchers monitoring the areas. This time was chosen as it corresponds to the lunchtime at the university when the selected locations experience the highest intensity of human presence throughout the day. Thirdly, the usage intensity of each zone was determined by dividing the number of people within that zone by the total number of people present in the entire selected locations during the same time period[5, 23].

2.4. Defining the layer of vulnerability (Phase 1c)

Individuals exhibit diverse perceptions of thermal comfort, leading to variations in their durability and vulnerability to thermal stress[5, 24]. To assess the vulnerability of people in this research, a questionnaire was employed. On March 14th, 2023, for location one, and on March 15th, 2023, for location two, questionnaires were administered between 12:00 and 13:00, to identify high thermal risk areas, it is necessary to generate three different layers within the same time period. Due to resource limitations, it was not possible to collect data from every individual present at the locations. However, efforts were made to conduct questionnaires with as many participants as feasible. To ensure a representative sample, participants of different genders and ages were selected (Appendix A, Table 1).

The questionnaires encompassed inquiries about participants' subjective thermal sensations, their perception of comfort, and their preferences regarding environmental factors such as humidity, wind speed, and air temperature. Moreover, relevant physical attributes including age, gender, clothing type, and level of activity were recorded. Additionally, the location of each participant was marked on the map to aid in identifying areas where individuals experienced uncomfortable conditions.

2.5. Future PET predictions for summer (Phase 2)

Due to predicted climate change and urban population growth worldwide, many previous researchers have analysed the future conditions of outdoor thermal comfort[25, 26]. The most commonly used index for analyzing outdoor thermal comfort in their research is the psychological equivalent temperature (PET) index[27, 28]. PET is considered a universal index that can be applied to both cold and hot thermal conditions, covering a wide range of thermal sensations or stress classifications[29].

In this study, after identifying outdoor areas with high thermal risk, the research proceeded to examine the future conditions of thermal comfort within these areas. NIWA (National Institute of Water and Atmospheric Research) prepared climate change projections and impacts for the Auckland Region, considering different future periods such as 2050 and 2080[30]. For this study, the summer of 2050 was selected as the midterm future scenario, while the summer of 2080 represented the far future.

To achieve this, climate weather files for Auckland in 2050 and 2080 were generated using the climate change world weather file generator (CCWorldWeatherGen), a tool that has been used in previous research studies with similar objectives[31, 32], and the assessment looks into climatic projections following RCPs of 8.5, which

represents the highest level of carbon emissions. In Auckland, for RCP8.5 at 2050, most of the region projects increases in annual Tmax of 0.75-1.25°C. At 2080, 2.75-3.25°C increase in annual Tmax is projected for most of the region. Subsequently, Envi-met was employed to simulate the microclimate conditions within the selected locations. The assessment of thermal conditions in future scenarios was conducted using the PET index, which served as a metric for evaluating thermal comfort.

2.6. Defining new scenarios (Phase 3)

After identifying the outdoor areas with thermal risk and analysing the future thermal comfort based on climate predictions, the study proceeded to design new scenarios aimed at reducing thermal stress in these areas. For this paper the future scenarios are limited to the use of greeneries, such as incorporating trees and green walls. The objective was to identify a new scenario for each location that would effectively mitigate thermal stress and enhance thermal comfort.

3.Results and Discussion

The methodology described in section 2 detailed the establishment of three separate layers: thermal stress, space usage intensity, and user vulnerability. These layers were developed to enable an effective assessment of the outdoor thermal risk present in specific locations. By overlaying these layers, it becomes feasible to visually identify and distinguish the various levels of outdoor thermal risk present within the chosen areas.

3.1. Preparing the layer of hazard (thermal stress)

We conducted field measurements from 8:30 to 16:30 on March 14th at location 1 (St. Paul Street) and on March 15th at location 2 (Hikuwai Plaza). The results obtained from the field measurements, including air temperature wind speed, and humidity were then compared with the corresponding data simulated by the Envi-met software.

Distribution of Field Measurements and Simulated Data by Envi-met software:

A statistical test called Shapiro-wilk test was applied to check whether the field measurements and simulated data by Envi-met in location 1 and location 2 follow a normal distribution. The Shapiro-Wilk test is especially useful when dealing with relatively small sample sizes ($n < 50$) [33]. The null hypothesis of the Shapiro-Wilk test is that the data in the sample is normally distributed. The results indicated that the field measurements and simulated data by Envi-met for air temperature (°C), humidity (%), and wind speed (m/s) in location 1 follow a normal distribution. However, in location 2, the field measurements and simulated data for air temperature (°C) and

humidity (%) also follow a normal distribution. Nevertheless, for wind speed, they do not follow a normal distribution, as the p-value is less than the significance level of 0.05. The mean and standard deviations are presented in Table 1.

Table. 1. Mean(μ) and standard deviation (σ) of field measurements and simulated data by Envi-met for Location1 (St. Paul Street) and Location2 (Hikuwai Plaza).

Location1			Location2		
Air Temperature (°C)					
Data	Mean(μ)	SD (σ)	Data	Mean (μ)	SD (σ)
Field Measurements	20.1	0.82	Field Measurements	19.14	0.65
Envi-met	19.55	0.85	Envi-met	19.30	0.73
Humidity (%)					
Data	Mean (μ)	SD (σ)	Data	Mean (μ)	SD (σ)
Field Measurements	70	5.68	Field Measurements	57.67	4.57
Envi-met	69.67	5.34	Envi-met	60	4.77
Wind Speed (m/s)					
Data	Mean (μ)	SD (σ)	Data	Mean (μ)	SD (σ)
Field Measurements	1.96	0.47	Field Measurements	1.07	0.76
Envi-met	2.43	0.58	Envi-met	1.43	0.1

Agreement between Field Measurements and Envi-Met Simulated Data:

R-squared is commonly used as a method to assess the agreement between measured data and simulated data. However, it is important to note that R-squared is not the only measure to consider when comparing measured and simulated data. Especially if the assumptions of linear regression are not fully met. The key assumptions are Linearity, independency of residuals, homoscedasticity, normality of residuals and no perfect collinearity between independent variables [34]. High R-squared values can occur even when the relationship between the datasets is spurious or coincidental. Therefore, it is essential to complement the R-squared evaluation with other methods, such as visualizations and statistical tests, to gain a comprehensive understanding of the agreement or differences between the measured and simulated data[35].

In this research, various methods were employed to assess these assumptions. Scatter plots to verify the linearity (Figure 3), Durbin-Watson statistical test to detect the presence of auto correlation in the residuals, Q-Q plot along with Shapiro-Wilk statistical test to check the normality of residuals, and finally the Residual vs. Fitted Values Plot to check homoscedasticity. No collinearity assumption does not apply to this problem as a single predictor variable is considered.

The results indicate that the assumptions of linear regression were satisfied for both Air Temperature and Humidity. Consequently, the R-squared metric was employed to assess the concordance between field measurements and the simulated data produced by Envi-met for these two parameters. The obtained R-squared values were 0.9537 for air temperature at Location 1 and 0.9497 at Location 2, revealing a robust alignment between the measured and simulated data at both sites. In terms of Humidity, R-squared values of 0.9629 (Location 1) and 0.9497 (Location 2) were observed, similarly affirming a strong agreement between the measured and simulated data at both locations. However, it should be noted that the assumption of normality of residuals was not satisfied for wind speed in either location (Figure 3).

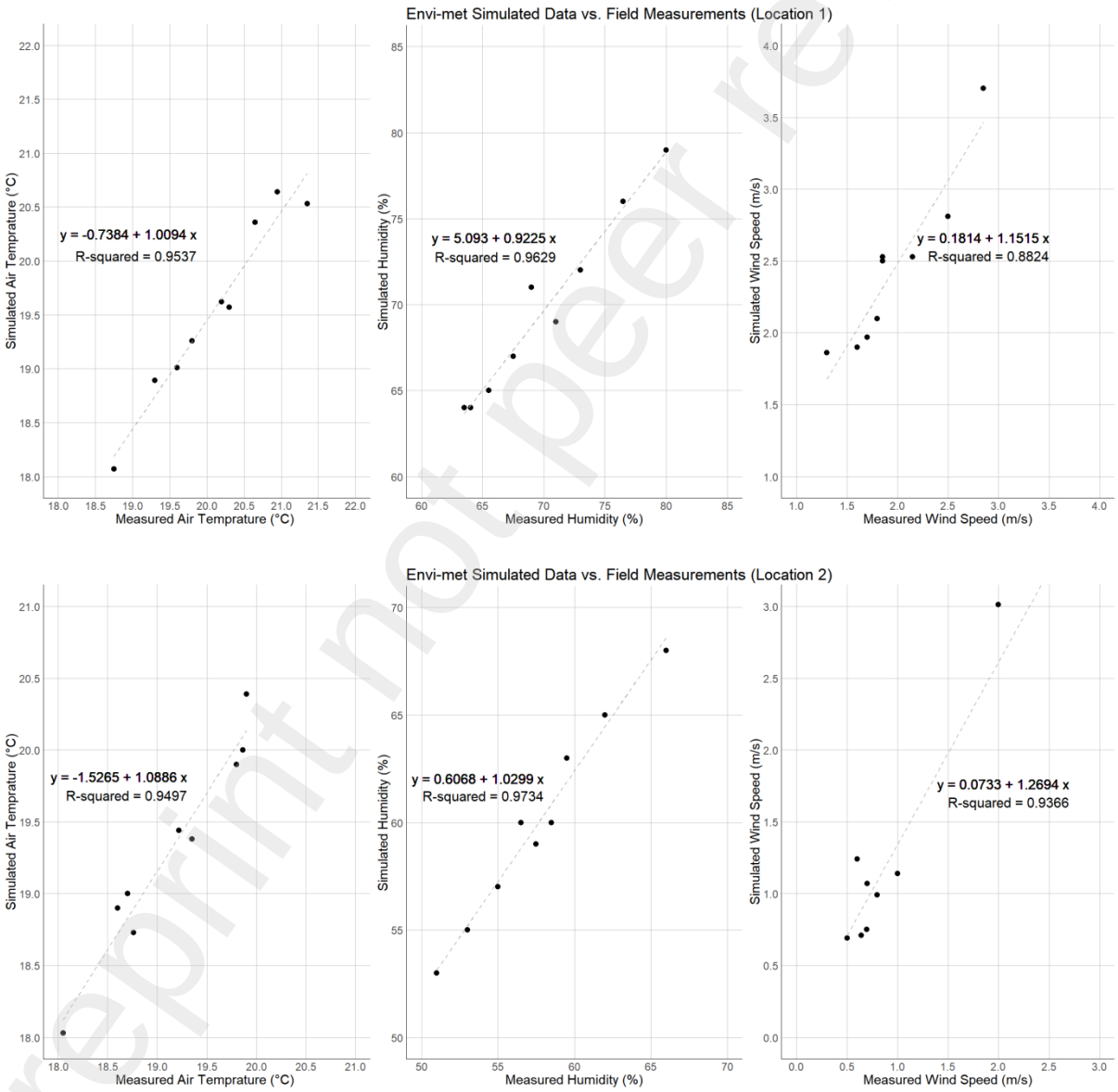

Figure 3. Scatter plot illustrating the measured and Envi-met simulated data points, along with the best fit line obtained from linear regression analysis.

To investigate these results further and since the linearity assumption is not met for wind speed, density plots were used to visualize the distribution of each dataset, and to provide insights into their shape, spread, and central tendency. By directly comparing the distributions, potential similarities or differences can be identified. As shown in the density plots (Figure 4), the distribution of field measurements and Envi-met simulated data for air temperature and humidity are highly similar. However, there are differences in the distribution of wind speed in both locations as expected. For both locations and for wind speed, the density plot of field measurements shows a prominent and higher peak, accompanied by a larger density value. Additionally, the shape of their peaks is notably narrower. These suggest the field measurements tight distribution around values 1.78m/s for location 1 and 0.67m/s for location 2. On the contrary, the density plots of the Envi-met simulated data take on a different appearance. Their peak is comparatively lower in density value, suggesting a lesser concentration of data points. Particularly, their peaks have shifted towards the right, suggesting a deviation from the central tendency observed in the measured data. The disparities in peak height, density value, and shape between the density plots reflects meaningful distinctions in the distribution patterns of the field measurements and Envi-met simulated data. These variations could potentially arise from underlying factors influencing the generation of the simulated data, emphasizing the importance of careful interpretation when comparing the measurements for wind speed.

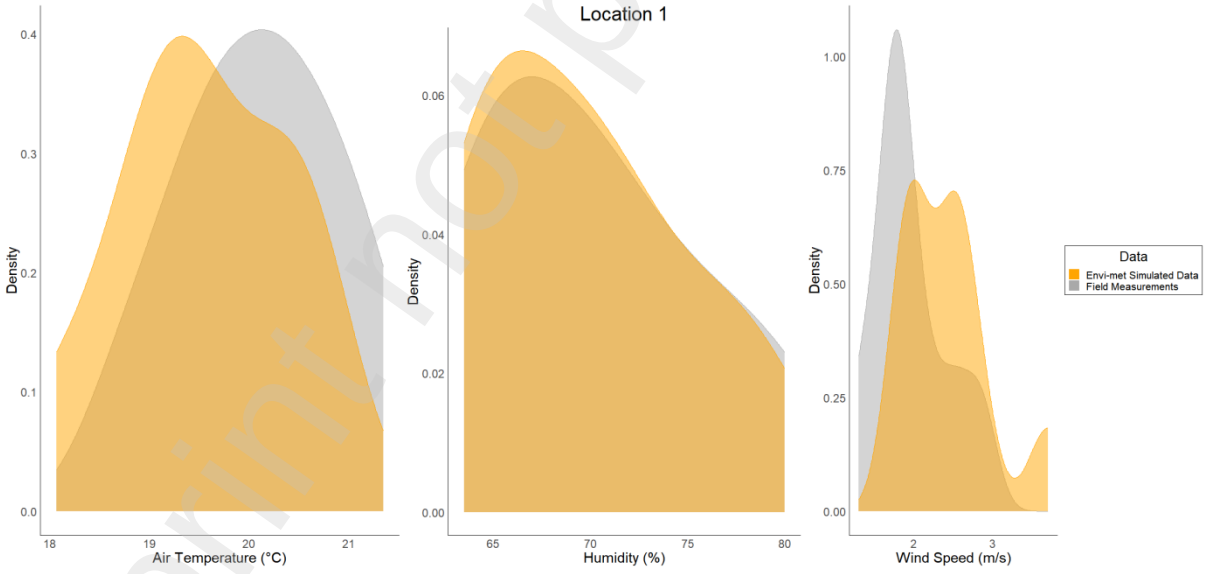

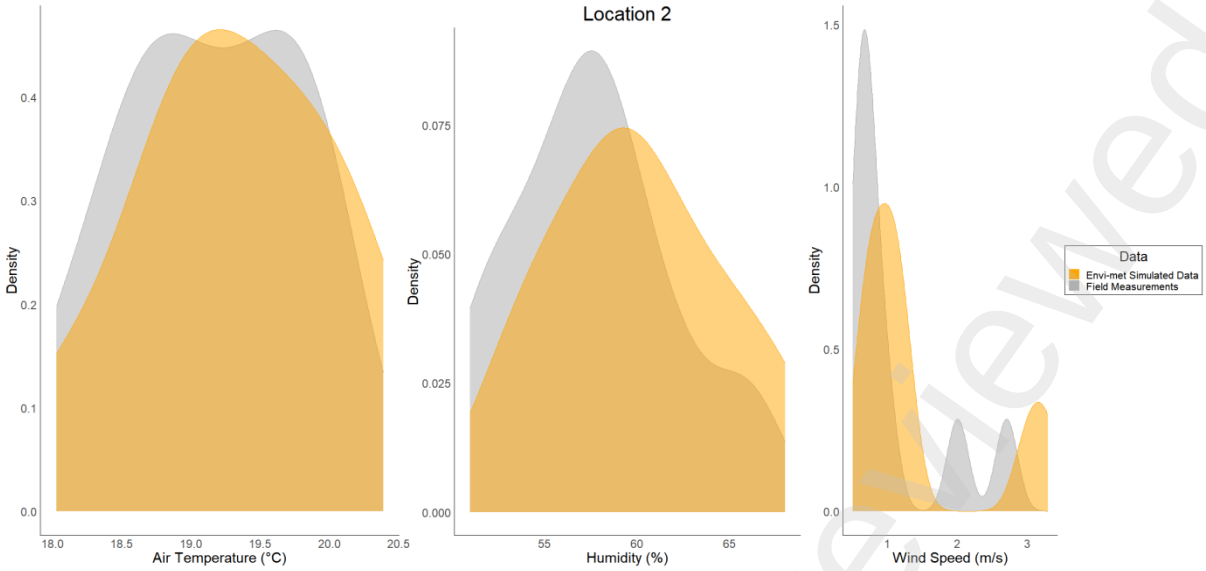

Figure 4. Density plots to compare distribution of field measurements and Envi-met simulated data in location 1 and location 2.

In this research, the period between 12:00 and 13:00 was selected for generating the PET map. This time frame was chosen because it coincides with the peak activity at the university, allowing us to observe and interact with a significant number of students to prepare the exposure and vulnerability layers. Based on field measurements and Envi-met results from 12:00 to 13:00 on March 14th, the average air temperature was recorded as 20.82 ℃, the average wind speed as 2.04 m/s, and the average humidity as 69.88% for location 1. As for location 2, the average air temperature, wind speed, and humidity during the period from 12:00 to 13:00 on March 15th were determined as follows: air temperature: 19.93 ℃, wind speed: 0.83 m/s, and humidity: 58.22% (Figure 5).

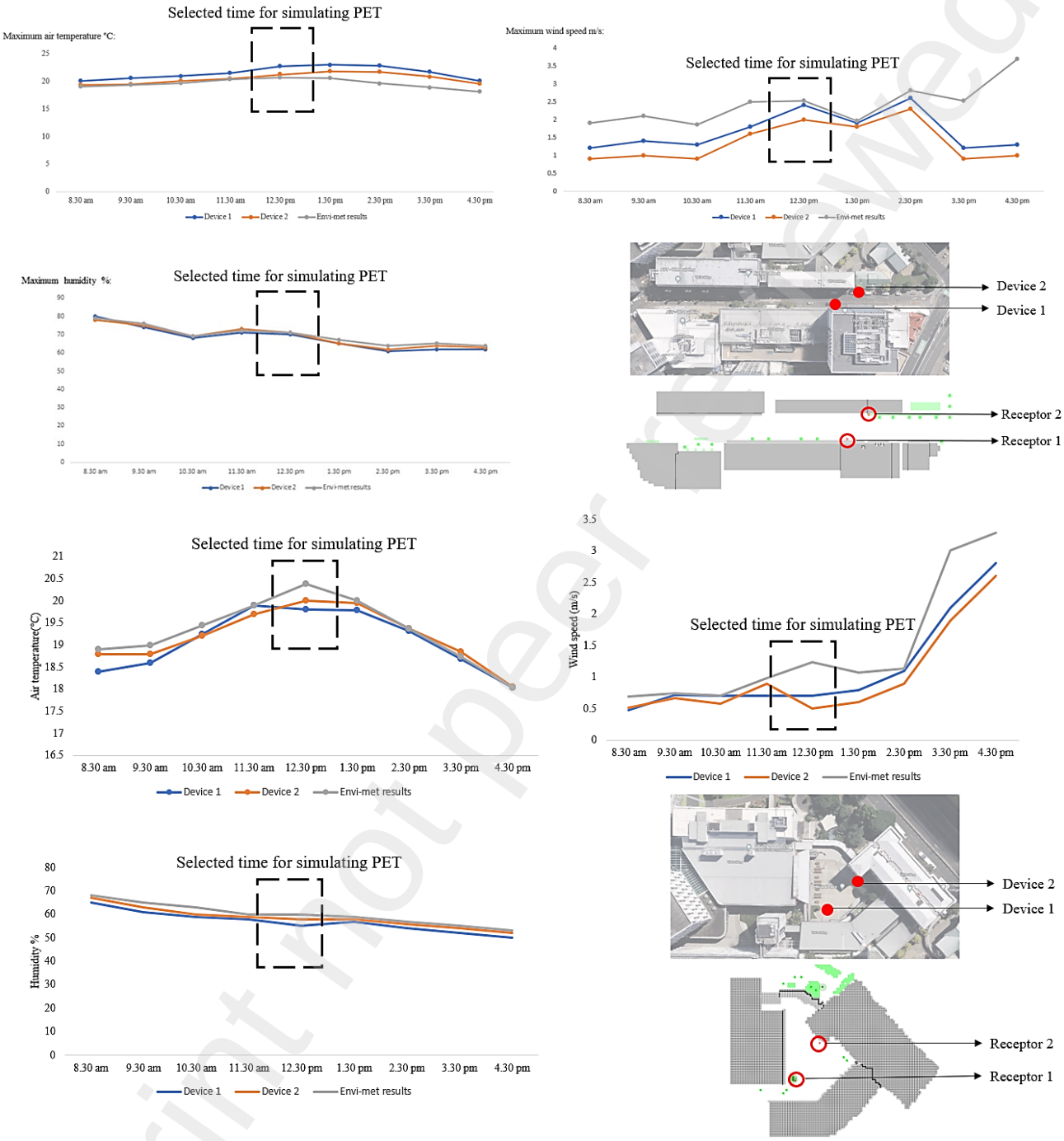

Figure 5. The results obtained from the field measurements and Envi-met simulation for air temperature, wind speed, and humidity on March 14, 2023, for location 1 and March 15, 2023, for location 2.

In this study, the term "hazard" refers to environmental thermal stress. Once the accuracy of Envi-met was determined, PET calculations were conducted to identify thermal stress areas in the selected locations. Auckland, characterized by a temperate climate according to the Koppen climate classification, has a comfortable PET range between 18°C and 23°C (Santos Nouri, Costa et al., 2018). Figure 6(a) illustrates the PET range for location 1 at 12:30 on March 14th. Based on the results, most parts of the location fall within the comfortable PET range of

19℃ to 22℃. Only a few areas within the location experience slight heat stress, with a PET range between 23℃ and 24.5℃.

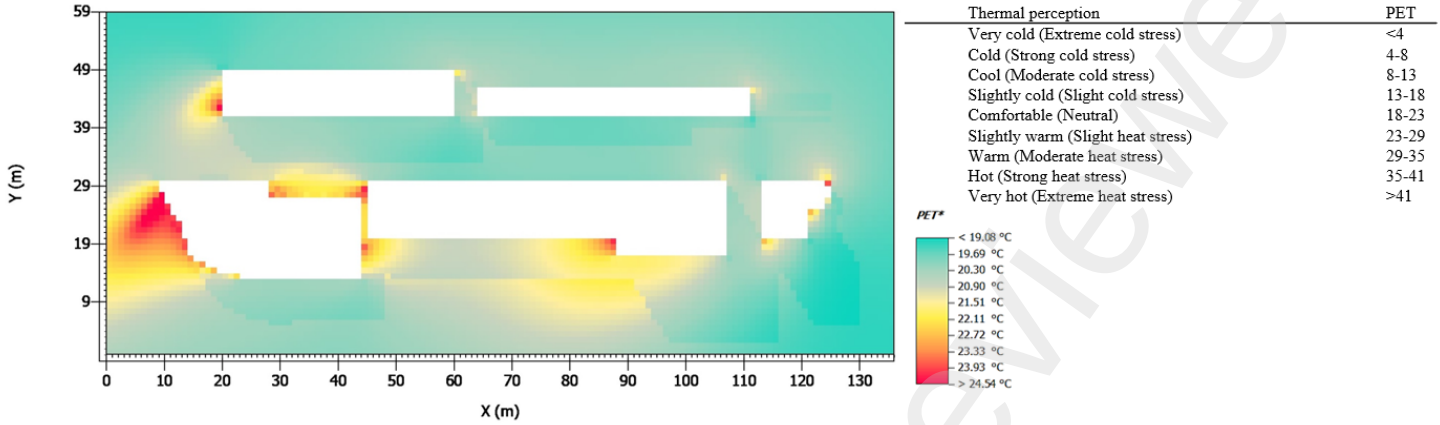

Figure 6(a). Layer of hazard for location 1 and categorization PET level for different thermal perception in a Cfb climate [29]

In the case of location 2, as depicted in figure 6(b), for 12:30 on March 15th, the majority of the selected area shows slightly warm conditions with slight heat stress, indicated by a PET range between 23℃ and 26℃.

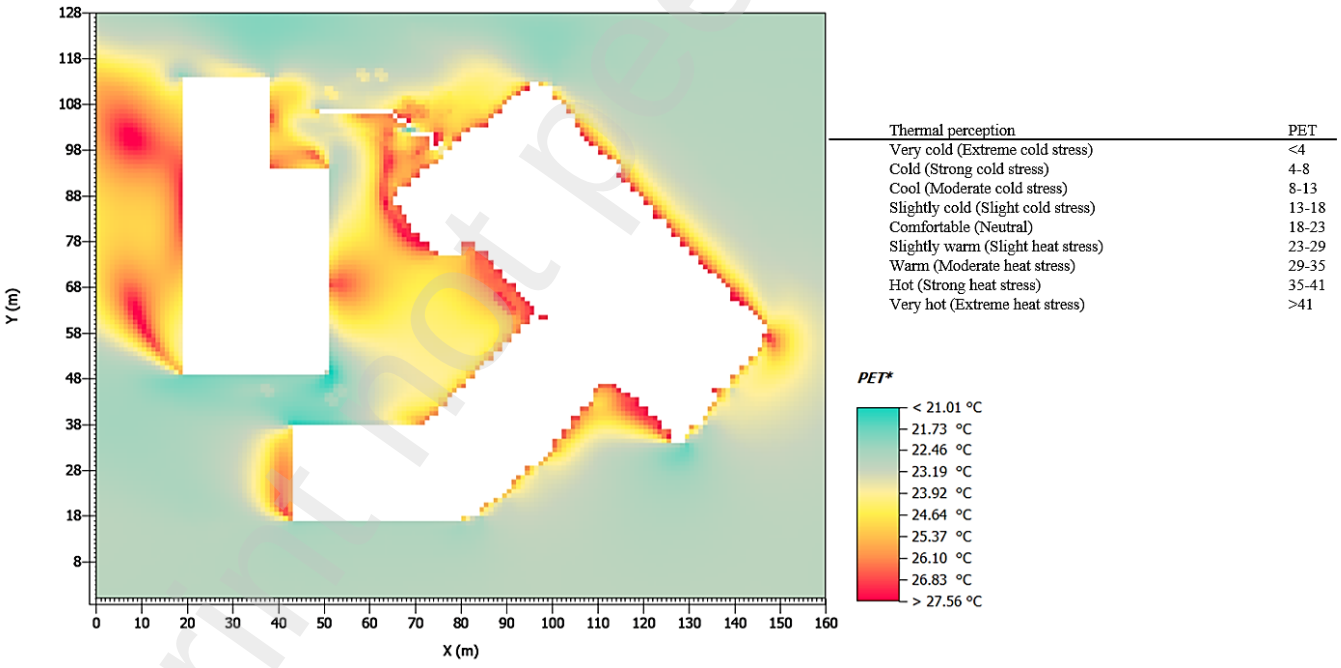

Figure 6(b). Layer of hazard for location 2 and categorization PET level for different thermal perception in a Cfb climate [29]

3.2.Preparing the layer of exposure (user intensity)

In the context of this study, the risk determinant "exposure" is defined as the intensity of space usage. It is understood that areas with higher intensity of space usage are associated with an increased likelihood of users being exposed to thermal stress[5].

In this research, for location 1 on 14 March 2023, we firstly divided the location into 3 zones and then counted the number of people in each zone[5] in 6 time sections, with a duration of 10 minutes each, from 12:00 to 13:00. We determined the usage intensity of people on the map, as shown in Figure 7(a). In total, there were 247 people in all zones combined for location 1, with 89 people in zone 1, 52 people in zone 2, and 106 people in zone 3 across all 6 time sections. By dividing the number of people in a selected zone by the total number of people in the location at a specific time, we obtained the usage intensity of that zone. As depicted in Figure 7(b), zone 3 had the highest exposure with a usage intensity of 0.42 in this location.

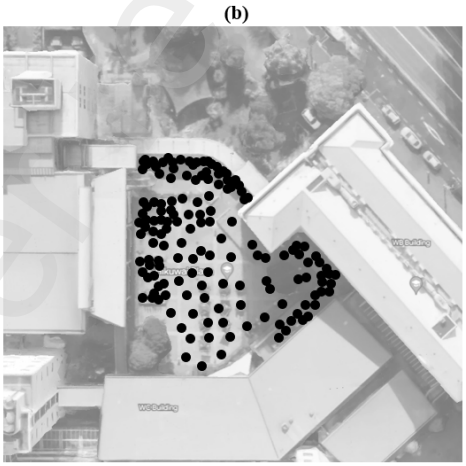

Time	Zone 1	Zone 2	Zone 3
12.00-12.10	10	5	15
12.10-12.20	13	7	13
12.20-12.30	20	9	14
12.30-12.40	22	11	28
12.40-12.50	14	8	22
12.50-13.00	10	12	14

Time	Zone 1	Zone 2	Zone 3	Zone 4	Zone 5
12.00-12.10	14	12	10	8	15
12.10-12.20	13	13	8	6	10
12.20-12.30	20	16	10	3	13
12.30-12.40	22	18	14	5	9
12.40-12.50	18	14	13	8	10
12.50-13.00	15	18	15	9	14

Figure 7(a). Layers of the number of people distribution (a) location 1, (b) location 2

The same method was employed to calculate the usage intensity of location 2 on 15 March 2023 from 12:00 to 13:00. We divided this location into 5 different zones, as shown in Figure 7(a). The results indicated that the total number of people in this location was 373, with 102 people in zone 1, 91 people in zone 2, 70 people in zone 3, 39 people in zone 4, and 71 people in zone 5. Based on Figure 7(b), zone 1 had the highest exposure with a usage intensity of 0.27 in location 2.

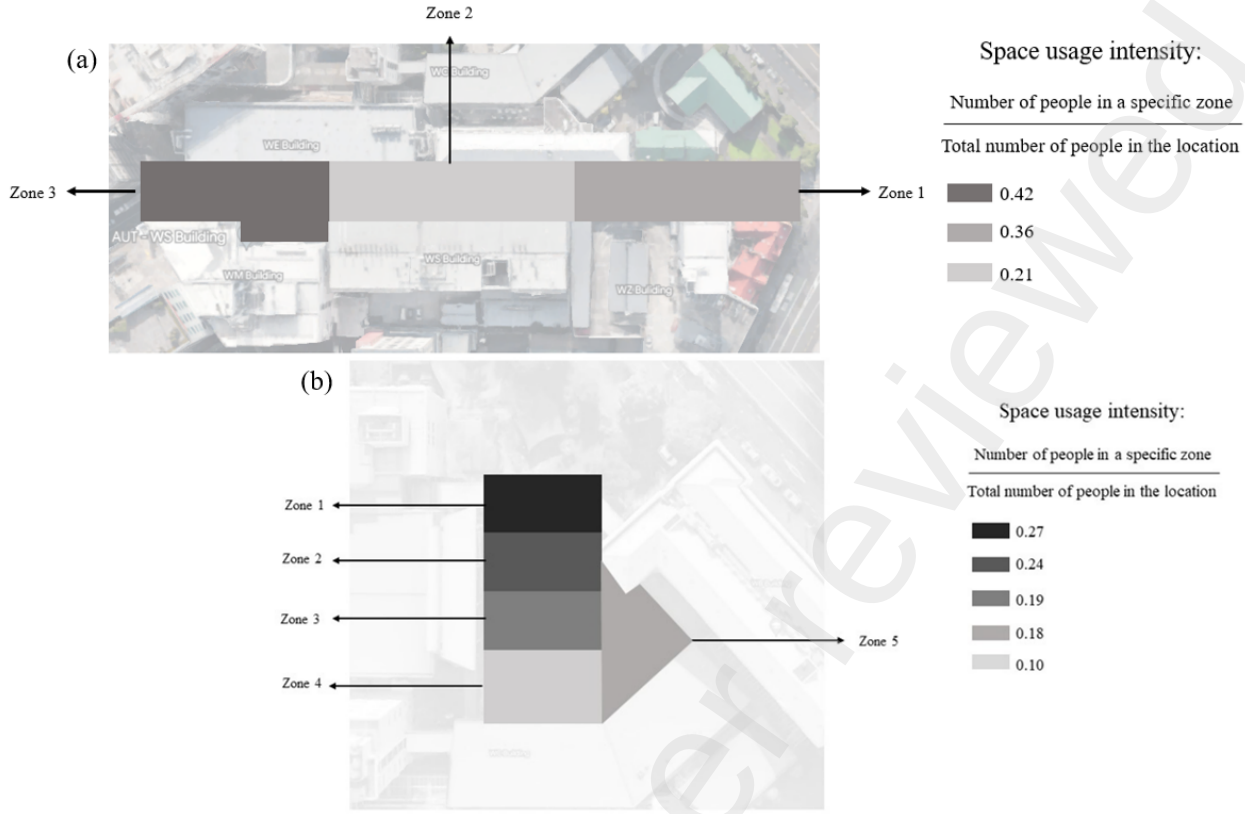

Figure 7(b). (a): Layer of exposure for location 1, (b): Layer of exposure for location 2

2.3.3.Preparing the layer of vulnerability

In this study, the risk determinant "vulnerability" is defined as the spatial distribution of user's adaptability capacity[5]. To achieve this objective, we used questionnaires to obtain people's perceptions of different weather conditions based on participants genders, activities, the period they have been living in Auckland.

From 12:00 to 13:00 on 14th March 2023, as we did not define a specific number of participants, our approach involved randomly selecting individuals within the designated timeframe. We aimed to ensure a diverse representation by including individuals of both genders and various age groups. Consequently, we were able to conduct the study with 30 participants at location one. As depicted in Figure 8(a), the study consisted of 18 females and 12 males, with approximately half of the participants falling within the 16 to 25-year age range. Additionally, we displayed the participants' locations on the map. Among the participants, 13 reported feeling slightly warm, while 7 indicated feeling warm. Concerning humidity, nearly 95% of participants perceived it as natural. As for wind speed, 18 participants reported feeling windy. Subsequently, when analysing the questionnaire responses, we identified the locations where individuals reported experiencing discomfort, which in this study referred to feeling slightly warm, warm, and windy. By aggregating these discomfort points, we generated a vulnerability layer.

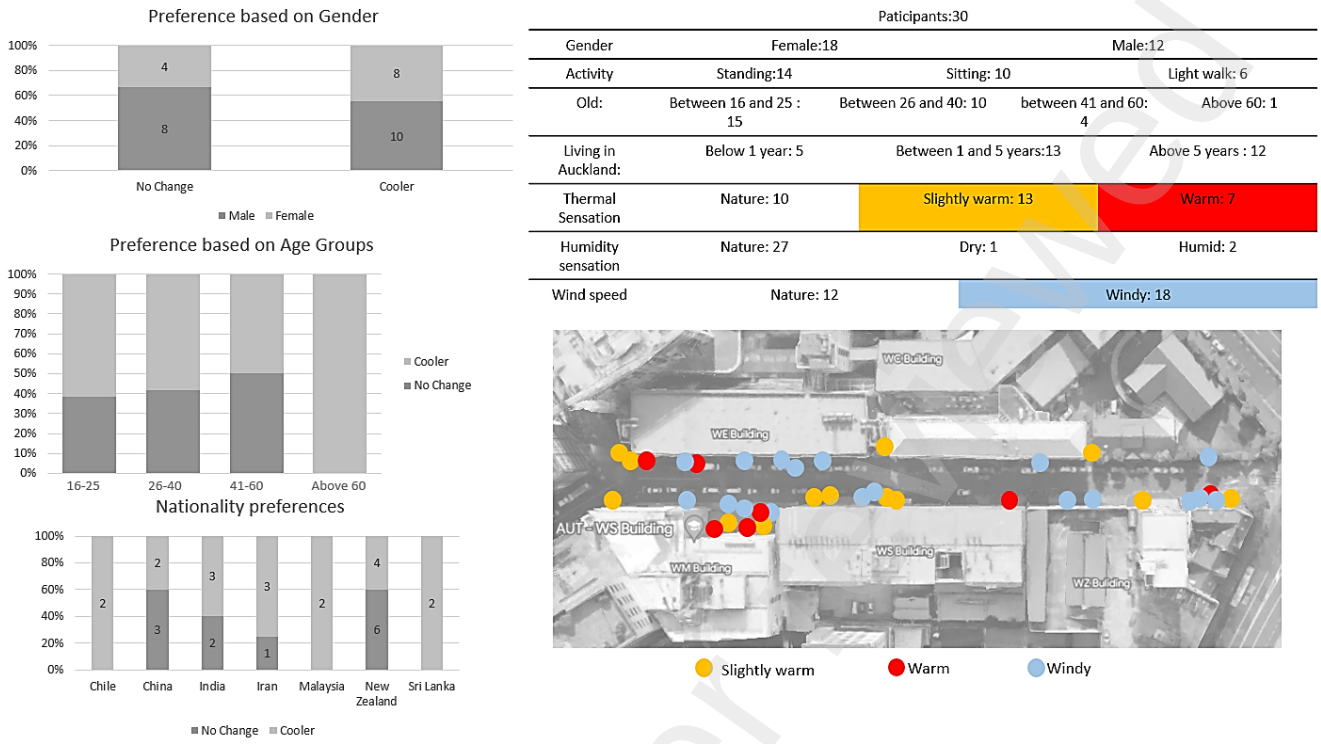

Figure 8(a). Layer of vulnerability for location 1

A similar approach was adopted for location two from 12:00 to 13:00 on 15th March 2023. In this case, we had 35 participants, including 17 females and 18 males. More than half of the participants fell within the 16 to 25-year age range. The questionnaire results indicated that 19 participants felt slightly warm, while 6 participants felt warm. Additionally, humidity was deemed acceptable by over 95% of the participants. Based on the questionnaire responses, 19 participants reported experiencing windy conditions. We marked the locations where people experienced discomfort on the map (Figure 8(b)). Therefore, these identified discomfort areas were considered vulnerability zones for two locations when creating the vulnerability layers.

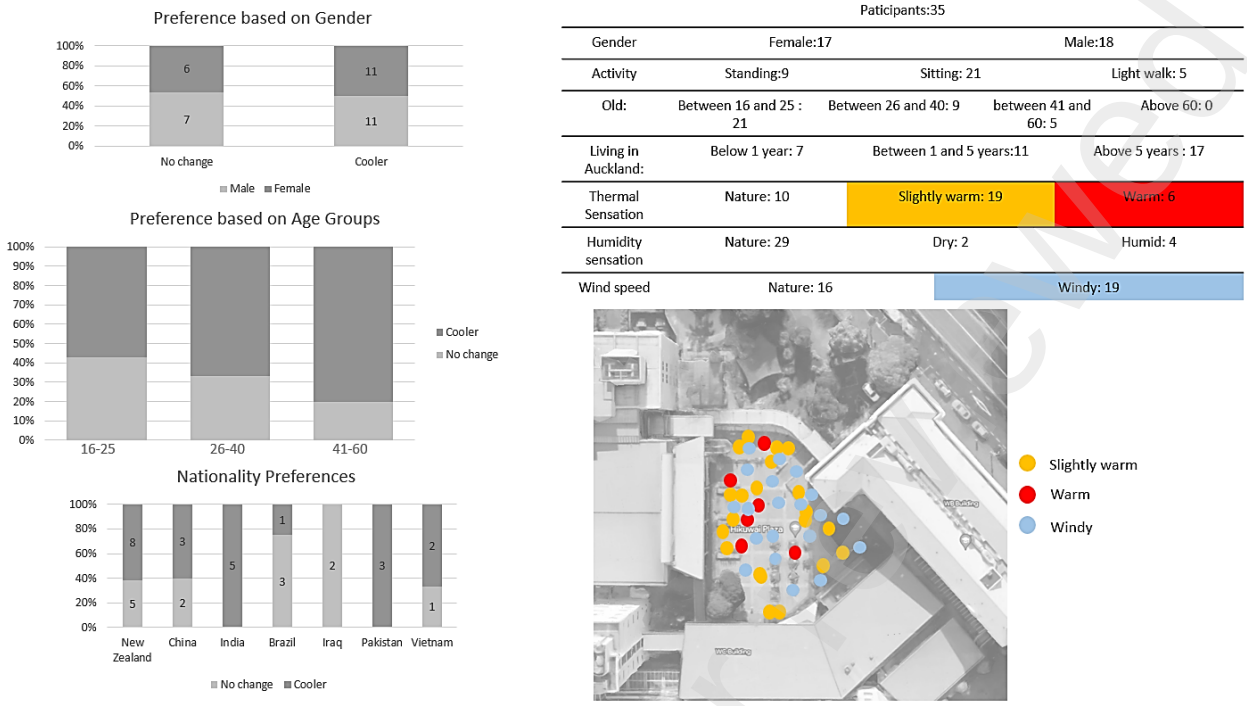

Figure 8(b). Layer of vulnerability for location 2

Relationship between Thermal Sensation and PET index:

In total, 167 questionnaire responses were gathered at location 1 on March 14, 2023, between 8:30 and 16:30. Additionally, 180 questionnaire responses were collected at location 2 on March 15, 2023, during the same time frame. Figure 9 illustrates a violin plot showcasing the distribution of PET indices across various thermal sensations reported by the participants. Each violin's outline signifies the frequency distribution of PET indices concerning different thermal sensations observed at the respective locations. The central white dot within each violin signifies the average PET index value. Accompanying the violins are box plots that encompass the interquartile range (IQR), while the horizontal lines within the boxes denote the median values. The higher peaks in the outlines indicate a more frequent occurrence of PET indices associated with warm thermal sensations in both locations. Conversely, for respondent groups experiencing other thermal sensations, the peak distribution concentrates around lower PET indices. Notably, there is not a distinct peak distribution for the PET index related to slightly cool thermal sensations at location 1. Every violin plot offers insight into the mean, maximum, and minimum PET index values, as well as the 25%–75% range of PET index distribution for different groups of respondents categorized by their thermal sensations. Specifically, at location 1, the mean PET index values are as follows: 19 for slightly cool, 21.88 for Neutral, 23.70 for slightly warm, and 24.52 for warm thermal sensations. In contrast, for location 2, the mean values are slightly elevated: 19.8 for slightly cool, 22.59 for Neutral, 23.77 for slightly warm, and 24.75 for warm thermal sensations.

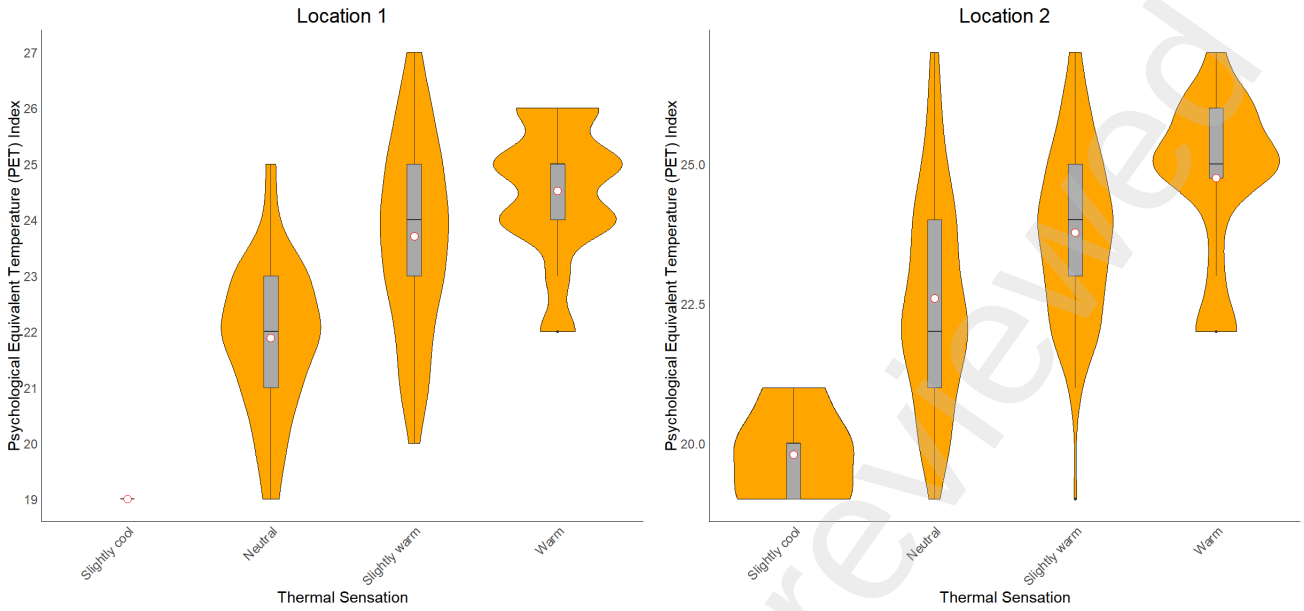

Figure 9. Distribution of PET index for outdoor thermal sensation votes.

Bubble plots are used to explore the relationship between respondents' thermal sensation and the PET index at Location 1 and Location 2 (Figure 10). As can be seen, there is a strong linear relationship between the mean respondents' thermal sensation and the PET index. This relationship can be modelled by linear regression where the regression equation represents the mean respondents' thermal sensation as a function of the PET index. It is mathematically represented as a linear function TSV = m*PET + c, where m is the PET coefficient or slope of the regression line, and c is the intercept, referred to as the deviation constant. The coefficient (m) quantifies the changes in thermal sensation per unit of PET change.

Regression equations representing the mean respondents' thermal sensation as a function of the PET index were obtained and expressed as follows:

(Location 1) TSV = 0.25 PET− 5.04 (R2 = 0.85) (e.q.1)

(Location 2) TSV = 0.18 PET− 3.56 (R2 = 0.83) (e.q.2)

In terms of outdoor thermal comfort, the PET coefficient is 0.25 in location 1 and 0.18 in location 2, corresponding to an increase of TSV by 0.25 and 0.18 units, respectively, for each 1°C increase in PET value.

These equations (e.q.1 and e.q.2) can be used to calculate the Neutral PET (NPET). The NPET refers to the PET index that corresponds to the mean vote of neutral on the thermal sensation scale (TSV = 0), i.e., the PET index

at which people feel neither cold nor warm. The NPET can be mathematically represented as NPET = -c/m, where 'c' is a constant, and 'm' is the slope. Using e.q.1 and e.q.2, we obtained NPET values of 19.96 °C at location 1 and 19.61°C at location 2. Notably, these results show a significant level of consistency.

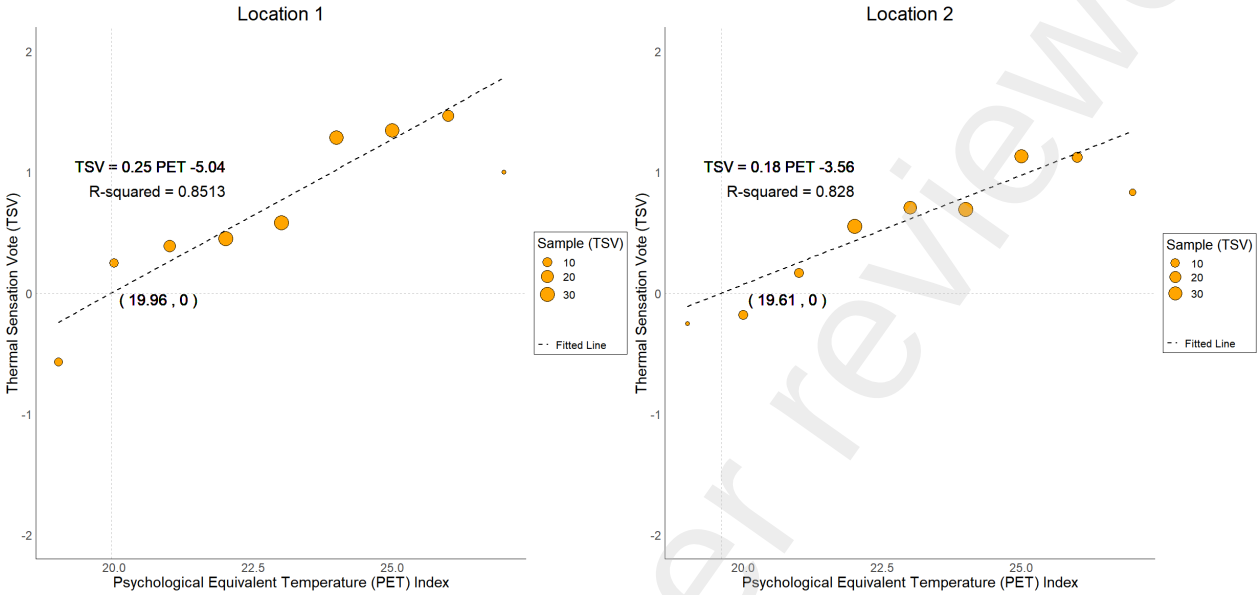

Figure 10. Bubble plot of the relationship between respondents' thermal sensation and the Psychological Equivalent (PET) index (Note: For TSV scale, -3, − 2, − 1, 0, 1, 2, and 3 represent cold, cool, slightly cool, neutral, slightly warm, warm, hot respectively).

Relationship between Thermal sensation and responses to questions:

Ordinal regression was utilized to explore how the thermal sensation experienced by the participants correlates with their answers on the questionnaire. This statistical method is employed to predict the behaviour of dependent variables or outcomes that have an ordinal scale, using a collection of independent variables or predictors. The dependent variable in this case involves categories with a specific order, while the independent variables can encompass both categorical and continuous factors [36]. The ordinal data was analysed with cumulative link models using the R package called ordinal [37]. When using ordinal regression to analyse the relationship between an ordinal outcome and categorical predictors, the model estimates how the odds of being in a particular category of the ordinal variable change based on the levels of the categorical predictors. It does this by estimating separate cumulative probabilities or odds for each category of the ordinal outcome, based on the different levels of the categorical predictors.

We examined the thermal sensation responses for all 347 questionnaires (across both sampling locations), which range from cold, cool, slightly cool, neutral, slightly warm, warm, and very warm. The independent variables were encoded according to the responses to the questions regarding gender, age, nationality, clothing, activity,

exposure to air conditioning before survey, and the length of time the respondent has lived in Auckland. In summary, this ordinal regression model suggests that age group and nationality are significant predictors of the thermal sensation.

According to table 2, the coefficient estimates for 41–60-year-olds is -1.0882 and the estimated odds ratio is approximately 0.3368. This means that the odds of being in a higher category for 41–60-year-olds are one-third (33.37%) of the odds of being in a higher category for 16–25-year-olds. This means that, on average, people in this age group (41–60-year-olds) are less likely to have a higher level of thermal Sensation vote (higher level of warmth) compared to the reference category (16–25-year-olds). Since the p-value (0.000886) is statistically significant, we have enough evidence to confidently conclude that there is a significant effect of age on thermal sensation. In other words, there is a meaningful and statistically significant difference in thermal sensation between people from different age groups.

Additionally, the coefficient estimates and the estimated odds ratio for New Zealand nationals found to be 0.5750 and 1.7777 respectively. The estimated odds ratio indicates that, on average, people who are originally from New Zealand have approximately 1.78 times higher odds of moving up one category in their thermal sensation compared to the reference category (those from other countries). In other words, on average, people from New Zealand are more likely to have a higher level of thermal Sensation vote (higher level of warmth) compared to people from other countries. Since the p-value (0.034) is statistically significant, we have enough evidence to confidently conclude that there is a significant effect of nationality on thermal sensation.

Table 2. Results of ordinal regression analysis of thermal sensation change with responses to questionnaire

	Coefficient (B)	95% CI		P-value	OR	95% CI	
Covariates		Lower bound	Upper bound			Lower bound	Upper bound
Gender							
Male	0.0923	-0.3196	0.5048	0.6607	1.0966	0.7264	1.6567
Female	Referent	-	-	-	-	-	-
Age group							
26-40	-0.0257	-0.4653	0.4136	0.9088	0.9747	0.6279	1.5123
41-60	-1.0882	-1.7385	-0.4526	0.000886***	0.3368	0.1758	0.6360
Above 60	0.4138	-0.9305	1.7660	0.5443	1.5125	0.3944	5.8472
16-25	Referent	-	-	-	-	-	-
New Zealand national							
Yes	0.5750	0.0435	1.1108	0.034444*	1.7772	1.0444	3.0369
No	Referent	-	-	-	-	-	-
Clothing							
2 layers	-0.0994	-0.6479	0.4482	0.7220	0.9054	0.5231	1.5655
>2 layers	-0.4849	-1.5425	0.5409	0.3580	0.6158	0.2139	1.7176
1 layer	Referent	-	-	-	-	-	-
Activity							
Light walk	-0.6300	-1.3142	0.0439	0.0682.	0.5326	0.2687	1.0449
Standing	-0.1208	-0.5522	0.3094	0.5822	0.8862	0.5757	1.3626
Sitting	Referent	-	-	-	-	-	-
Indoor air conditioning before survey							
Yes	-0.2817	-0.7115	0.1456	0.1971	0.7545	0.4909	1.1568
No	Referent	-	-	-	-	-	-
Period living in Auckland							
1-5 years	0.5222	-0.0675	1.1167	0.0835.	1.6857	0.9348	3.0548
Above 5 years	-0.1272	-0.7643	0.5111	0.6954	0.8806	0.4657	1.6672
Below one year	Referent	-	-	-	-	-	-

Significant codes: 0 '***' 0.001 '**' 0.01 '*' 0.05 '.' 0.1

3.4.Identifying thermal risk areas

As outlined in section 2, the layers depicting the distribution of thermal stress, space usage intensity, and user vulnerability are combined through the superimposition process, utilizing the red-scale brightness levels from each layer map. This integration is visually presented in Figure 11(a) and Figure 11(b). In this representation, areas characterized by brighter red-scale indicate a lower level of risk, while regions with darker red-scale indicate a higher potential for thermal risk.

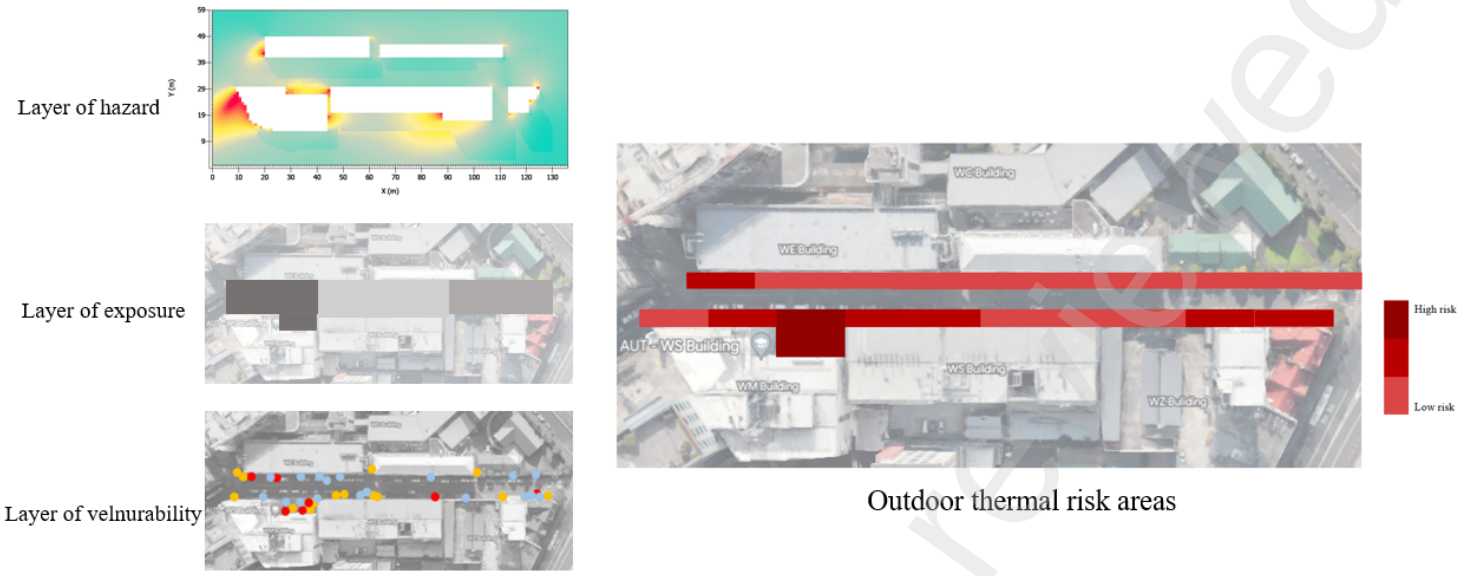

Figure 11(a). The construction of thermal risk map for location 1

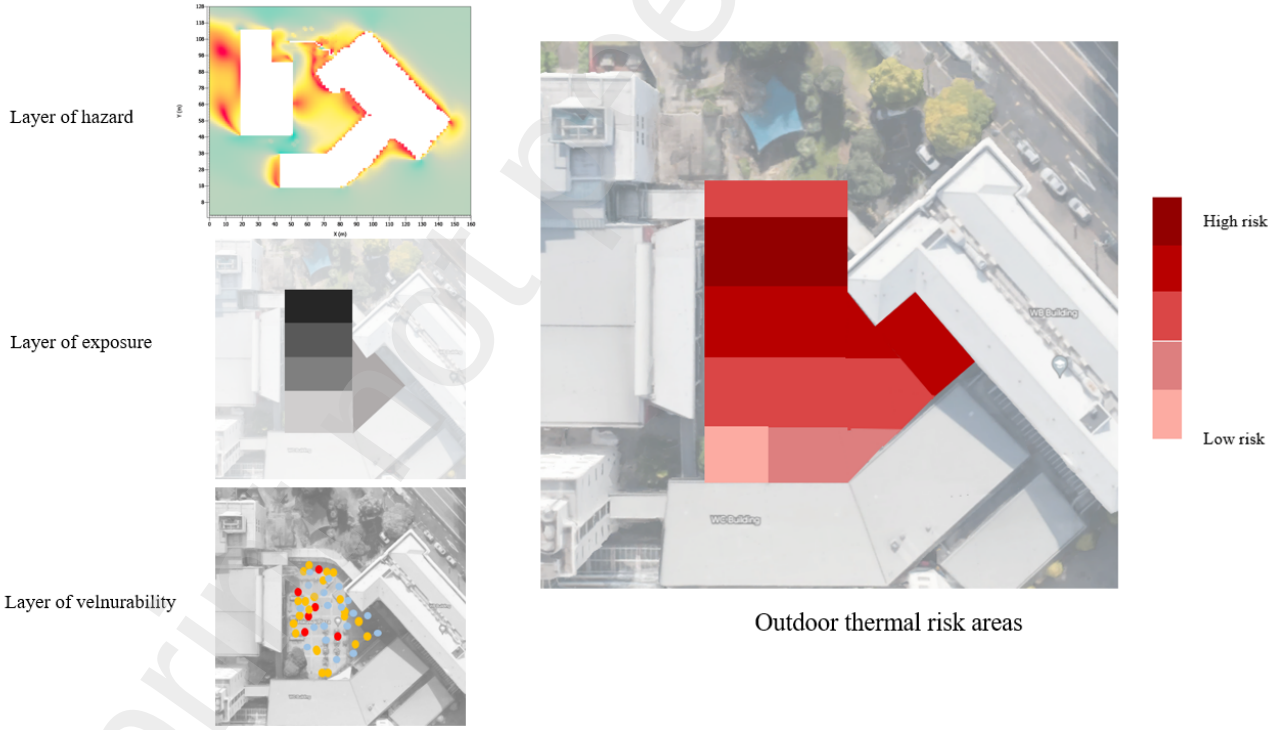

Figure 11(b). The construction of thermal risk map for location 2

4.4. Investigating future conditions for years 2050 and 2080 at outdoor thermal risk areas

To gain a preliminary understanding of the future trend of thermal comfort within the identified thermal risk areas, we conducted calculations to estimate PET levels for the summers of 2050 and 2080. To achieve this, we generated future climate scenarios using CCWorldWeatherGen. This tool, based on Microsoft Excel, enables us to generate

climate change weather files that can be used in building performance simulation programs. It transforms 'present-day' EPW weather files into climate change EPW weather file[38], which is compatible with Envi-met for simulating outdoor thermal comfort.

Based on the EPW weather files generated for summers 2050 and 2080 and by comparing the data with the EPW file of 2023, it is demonstrated that the average air temperature for March 2050 is projected to increase by approximately 0.5°C to 2°C, and for March 2080, the air temperature is expected to rise by approximately 1.7°C to 4.2°C.

The climate change projections and impacts for the Auckland region for RCP 8.5 are based on plans generated by the National Institute of Water and Atmospheric Research (NIWA). According to these projections, in summer 2050, the air temperature is predicted to increase by 0.75°C to 1.5°C, and by 2.5°C to 4°C in 2080.

By comparing the results of the generated air temperature in Summer 2050 and 2080 from CCWorldWeatherGen with the NIWA data, it can be concluded that the predicted air temperature using CCWorldWeatherGen is relatively accurate, with a difference of approximately 0.5°C compared to the NIWA data. Therefore, the generated data has been validated for our research, and we have utilized it as input weather data for simulating future PET in Envi-met.

The results, illustrating the differences in PET between the time periods, are presented in Figure 12 for location 1 and Figure 13 for location 2. Based on the simulations, we can conclude that in the future, people will face more thermal discomfort in thermal risk areas. To be more precise, the results from the Envi-met for location 1 indicate that the average PET in March 2023 is approximately 22.11°C. This is projected to increase to 24.39°C in 2050 and 26.45°C in 2080. Similarly, for location 2, the average PET for thermal risk areas in March 2023 is 23.92°C, which is expected to rise to 25.58°C in 2050 and 27.69°C in 2080.

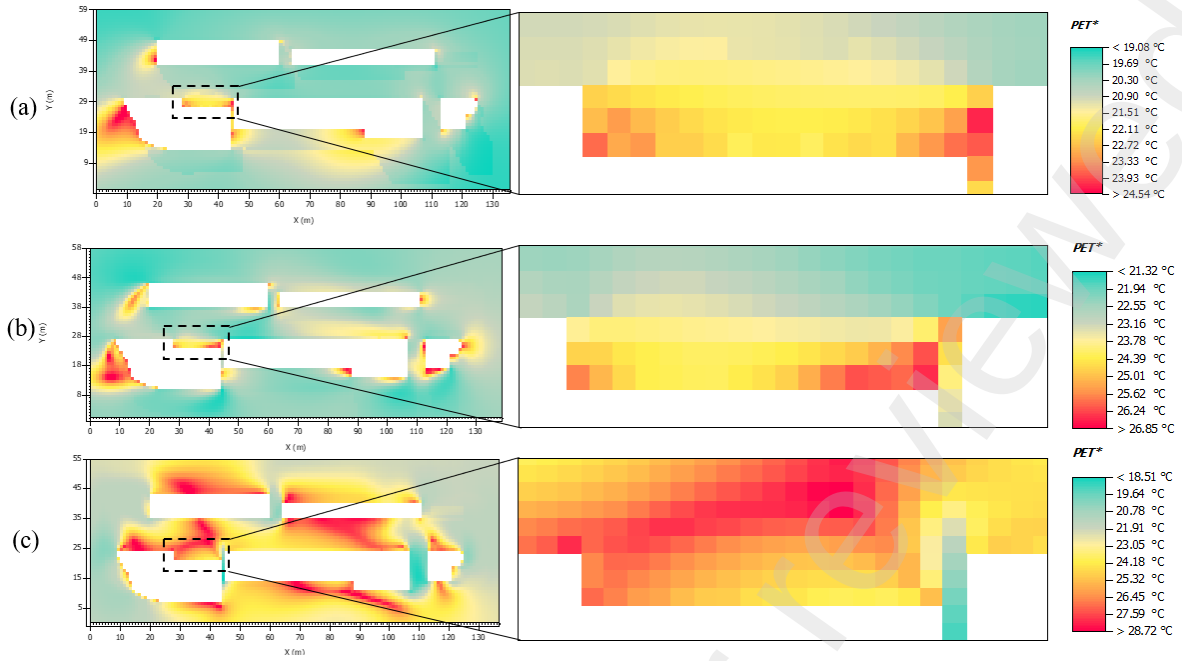

Figure 12. The PET levels and percentage for the areas with high outdoor thermal risk in location 1, depicting the years 2023(a), 2050(b), and 2080(c)

Based on Figure 12, the thermal risk area of location one in 2023 shows that PET exceeding 25℃ constitutes only about 5% of the total area. However, this percentage is projected to increase to more than 60% in 2050 and 2080. To provide more specific details, by 2050, the thermal risk area will experience PET between 25℃ and 27℃ in approximately 50% of the spots. By 2080, PET exceeding 27℃ will be observed in approximately half of the spots within the thermal risk area.

According to Figure 13, in 2023, approximately 30% of the thermal risk area in location 2 experiences PET exceeding 25℃. This percentage is projected to increase to 80% in 2050 and approximately 90% in 2080. By 2050, around 70% of the spots will experience PET between 25℃ and 27℃, while in 2080, nearly 30% of the spots will face PET exceeding 27℃, and only 10% of the area will have PET between 23℃ and 25℃.

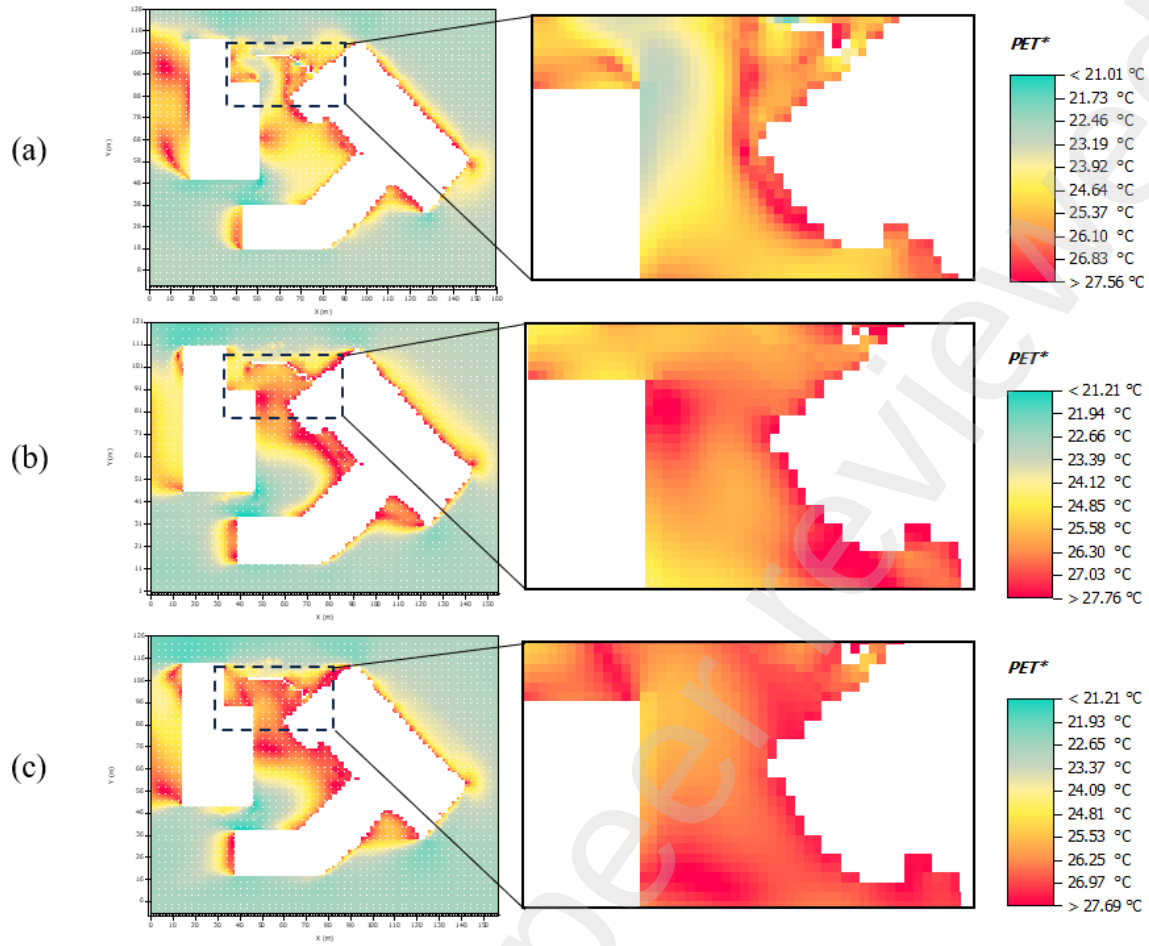

Figure 13. The PET levels and percentage for the areas with high outdoor thermal risk in location 1, depicting the years 2023(a), 2050(b), and 2080(c)

4.5.Results of mitigation strategy scenarios

After identifying thermal risk areas and analysing the future thermal conditions in these areas, we attempted to define new scenarios for mitigating thermal stress. In the first stage, we thoroughly categorized the features of the thermal risk areas and sought the best approach based on the specific characteristics of each location to optimize the thermal conditions in those areas. The thermal risk area of Location 1 (St. Paul Street) pertains to the outdoor area of the Art and Design Building of AUT, while for Location 2 (Hikuwai Plaza), it refers to the central area of the plaza. All the features of the thermal risk areas are presented in Table 3.

Table 3. Features of thermal risk areas

	Outdoor thermal risk area of location 1	Outdoor thermal risk area of location 2

Aerial image		
Image		
Geometry features	This area has a rectangular shape and is located in front of a 28-meter-high building. The width of the thermal risk area is approximately 14 meters, resulting in an aspect ratio of 2.	This area is situated between two buildings with heights of 24 and 16 meters, respectively. The thermal risk area has an approximate width of 25 meters, resulting in an aspect ratio of 0.8.
Material features	Building materials: Concrete, Steel, Glass Pavement materials: Light concrete, and asphalt	Building materials: Concrete, Steel, Glass Pavement materials: Light concrete
Greenery Features	There are four young trees and limited grass coverage in the area.	None

In order to establish future scenarios, an analysis was conducted on the conditions of outdoor thermal risk areas. At this stage, we decided to analyse the impacts of greenery on thermal risk areas, as the lack of sufficient green cover is evident in both thermal risk areas. Moreover, the preferences of the participants were taken into account through questionnaires, where more than half of the 65 respondents (30 participants in location 1 and 35 participants in location 2) expressed their support for enhancing vegetation cover. Consequently, this approach was further investigated. Table 4 provides the locations and features of the selected scenarios.

Table 4. Features of future scenarios for high thermal risk areas

To address the high thermal risk in Location 1, it is proposed to replace the concrete wall of the building with green walls. The features of the green wall is as follows: Green + mixed substrate Plant thickness: 0.30 m Substrate thickness: 0.15 m Greening properties: LAI [m^2,m^2]: 1.5 Leaf angle distribution: 0.5 Substrate properties: Emissivity: 0.95 Albedo: 0.30 Air gap between substrate and wall (m): 0.10	
Six trees, positioned at a distance of 4 m from each other, were considered in the high thermal risk areas of location 2. The features of the trees are as follows: Foliage shortwave albedo: 0.18 Foliage shortwave transmittance: 0.30 Leaf emissivity: 0.96 Crown top height: 3.5 m Leaf type: Coniferous Height: 5 m Width: 2.25 m	

For the outdoor thermal risk area in location 1, the existing concrete wall of the building was replaced with a green wall. Regarding the outdoor thermal risk areas in location 2, the impact of tree planting was analysed. The outcomes of these new scenarios, measured in terms of PET, are presented in Figures 14 and 15.

Figure 14 illustrates that the current average PET in the highest thermal risk area of location one is 22°C, which can be reduced to an average of 20°C by replacing the concrete wall with a green wall. In the case of location two, the current average PET in the highest thermal risk area is 25°C, and it can be decreased to 22°C through the implementation of tree planting (Figure 15).

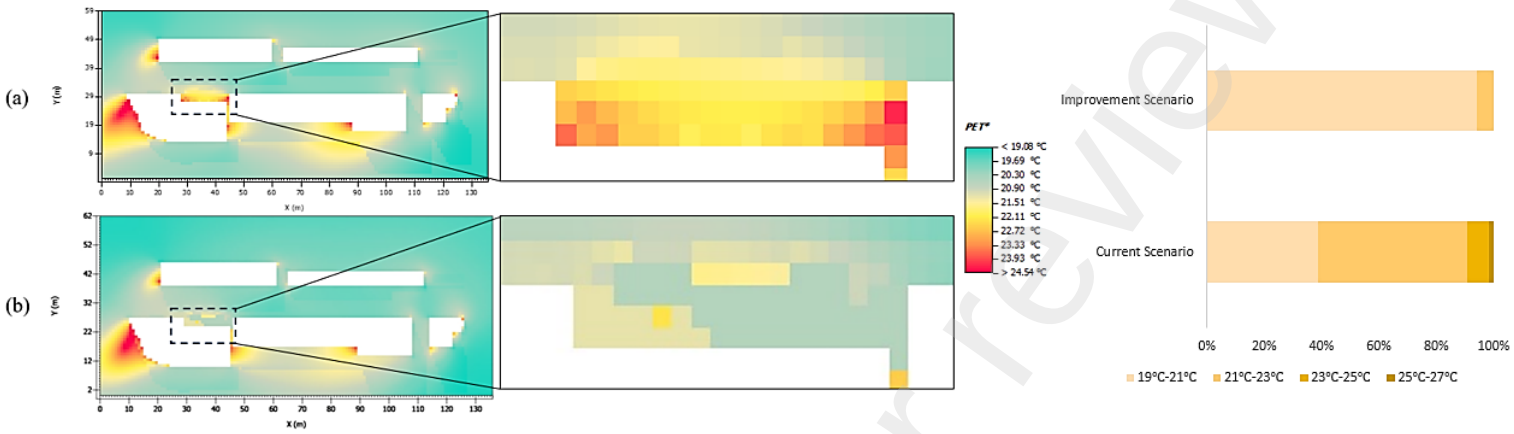

Figure 14: (a) PET levels of outdoor thermal risk area at location one under the current scenario. (b) PET levels of outdoor thermal risk area at location one under the defined scenario

Based on Figure 14, in the current situation of the thermal risk area in location one, nearly 10% of the area experiences PET exceeding 23°C. However, by replacing a concrete wall with a green wall, the percentage of the area with PET between 19°C and 21°C increases significantly to over 90%.

Regarding location 2, as shown in Figure 15, in the current scenario, around 80% of the spots within the thermal risk area experience PET exceeding 23°C. However, by planting trees, approximately 50% of the area will have PET levels below 23°C, and no spots will experience PET levels above 27°C.

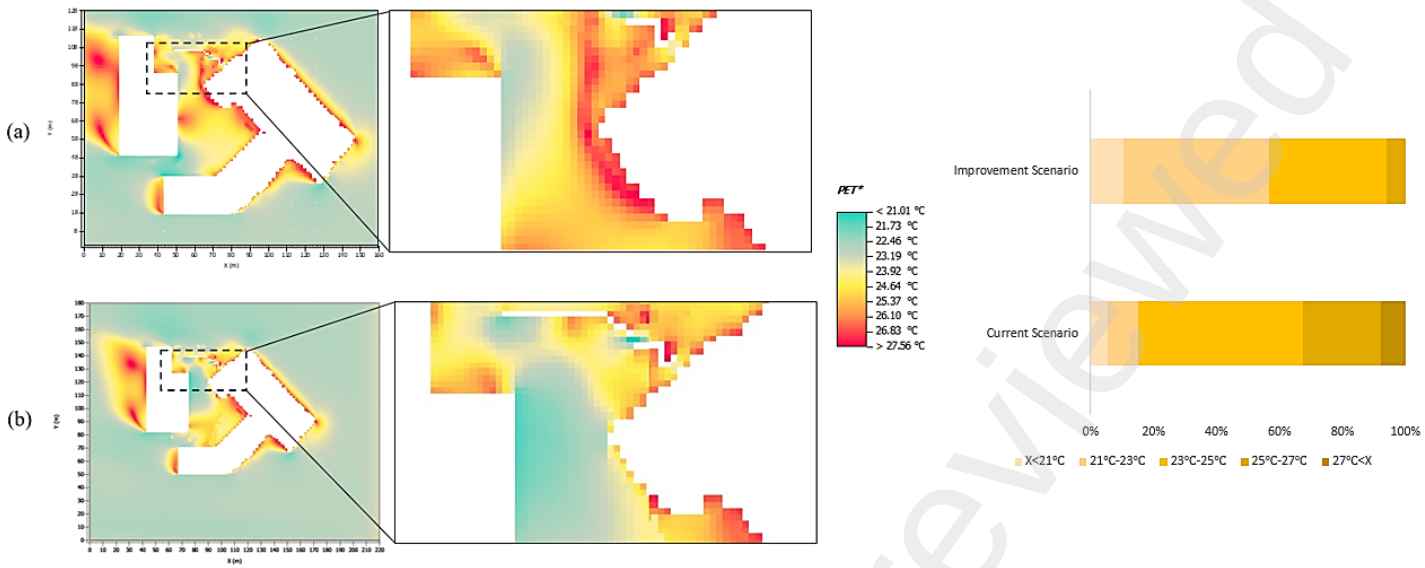

Figure 15: (a) PET levels of outdoor thermal risk area at location two under the current scenario. (b) PET levels of outdoor thermal risk area at location two under the defined scenario

Based on the observed changes in climate patterns and the results obtained in this study, which emphasize the projected increase in thermal stress within thermal risk areas in future summers, as well as the positive impact of greenery in reducing current PET levels in high-risk areas, we hypothesize that incorporating greenery in the identified thermal risk areas would be an effective approach for enhancing outdoor thermal comfort in the future as well.

4. Discussions and limitations of the study

In this study, aimed at identifying thermal risk areas, we overlaid the hazard, exposure, and vulnerability layers. This involved identifying areas with PET values exceeding 23°C and a high exposure of people, reporting the highest discomfort. For each location identified as having a high thermal risk, we defined specific strategic scenarios to mitigate thermal stress. These scenarios address both the current situation and future conditions based on predicted climate patterns. This research is a crucial component of our comprehensive study, aiming to validate the effectiveness of the proposed approach and gain valuable insights through a focused case study. However, it is important to acknowledge a limitation of this investigation, which lies in its narrow focus on a specific hour during a summer day for identifying outdoor thermal risk areas within the selected location. To address this limitation, our future efforts will involve expanding the scope of our research to cover longer time periods, allowing us to evaluate thermal risks during both hot and cold periods. This expansion will entail conducting PET simulations over multiple days to identify areas of thermal discomfort. Furthermore, we plan to enhance our data collection by involving a larger and more diverse group of participants. This will enable us to develop

comprehensive exposure and vulnerability layers, providing a more comprehensive understanding of the thermal risks.

While our current study primarily emphasizes the assessment of thermal risks during hot periods, our subsequent investigations will extend to examining future climate scenarios, encompassing both hot and cold periods. This comprehensive approach will help us understand the varying dynamics of thermal discomfort in different climatic conditions. Moreover, our focus on defining new scenarios has been centred around investigating the impact of greenery in mitigating outdoor thermal risks. However, our future research will explore a wider range of scenarios, aiming to identify the most optimal approaches for mitigating thermal risks. It is crucial to emphasize that the current scenario presented in this research serves as a preliminary suggestion and should not be considered the definitive or ideal solution.

5. Conclusions

Due to urbanization and predicted climate change, the study of microclimate and outdoor thermal comfort has gained popularity in recent decades. However New Zealand major cities like Auckland and Wellington are relatively understudies. In this study, our method was to identify the thermal risk areas in the city campus of Auckland University of Technology in New Zealand. Our analysis focused on the period of 12:00 to 13:00 on the 14th and 15th of March 2023. Furthermore, we aimed to examine the future thermal patterns in these areas by simulating the Physiologically Equivalent Temperature (PET) for the summers of 2050 and 2080. Finally, we aimed to propose new scenarios for optimizing thermal stress in these areas.

After identifying the thermal risk areas by overlaying the three layers, we utilized future climate data to predict the PET conditions. The results indicated that in location one, the projected PET would reach 24.39°C in 2050 and 26.45°C in 2080. Similarly, in location two, the PET was projected to increase to 25.58°C in 2050 and 27.69°C in 2080. Finally, we analysed new scenarios for both locations to mitigate thermal stress in the identified thermal risk areas by introducing greenery. The results demonstrated that for location one, replacing the concrete wall with a green wall resulted in an average PET reduction of 2°C, decreasing from 22°C to 20°C. In location two, the planting of trees resulted in an average PET reduction of 3°C, decreasing from 25°C to 22°C.

In conclusion, while assessing the level of outdoor thermal comfort in various locations has been a popular focus among researchers, our study aimed to identify outdoor thermal risk areas not only by identifying locations with high thermal stress, but also by considering the presence of people and their reported discomfort in these areas.

Given the predicted climate change and its global significance, it is crucial to take action regarding outdoor spaces frequently used by people that are susceptible to thermal risks.

Based on the findings of our research, the following conclusions can be drawn:

- Under the current scenario and in the future, the identified thermal risk areas will experience higher thermal stress. The range of thermal stress in these areas is projected to increase by approximately 2°C in 2050 and 4°C in 2080.
- Considering the simulation results and predicted climate patterns, it is expected that Auckland will encounter an increase in the number of outdoor thermal risk areas during summers in the future.
- Based on the results of questionnaires, age group and nationality are significant predictors of the thermal sensation.
- The results of the questionnaires conducted in Auckland reveal that high wind speed is as concerning as air temperature during summer, leading to discomfort in outdoor spaces. This aspect warrants further analysis in future studies.
- The simulation results indicate that greenery, specifically trees and green walls, have a significant impact in reducing PET levels in the identified thermal risk areas of Auckland during summer. Future researchers can leverage greenery to enhance outdoor thermal comfort in the urban context of Auckland.

Our study highlights the importance of addressing outdoor thermal risks in urban areas, provides insights into the impact of climate change on thermal stress, and suggests the implementation of greenery as a potential solution to improve outdoor thermal comfort in Auckland. The methods and findings presented in this study are expected to provide valuable insights for urban planners and architects in identifying thermal risk areas in various urban contexts and in implementing strategies to mitigate thermal stress. These efforts can contribute to improving the liveability of outdoor spaces in cities.

Acknowledgements

This research did not receive any specific grant from funding agencies in the public, commercial, or not-for-profit sectors.

Data availability statement

The authors confirm that the data supporting the findings of this study are available within the article.

References

1. Zhou, X. and H. Chen, Impact of urbanization-related land use land cover changes and urban morphology changes on the urban heat island phenomenon. Science of the Total Environment, 2018. 635: p. 1467-1476.
2. Heris, M.P., A. Middel, and B. Muller, Impacts of form and design policies on urban microclimate: Assessment of zoning and design guideline choices in urban redevelopment projects. Landscape and Urban Planning, 2020. 202: p. 103870.
3. Natanian, J., O. Aleksandrowicz, and T. Auer, A parametric approach to optimizing urban form, energy balance and environmental quality: The case of Mediterranean districts. Applied Energy, 2019. 254: p. 113637.
4. Lin, T.-P., A. Matzarakis, and R.-L. Hwang, Shading effect on long-term outdoor thermal comfort. Building and environment, 2010. 45(1): p. 213-221.
5. Huang, K.-T., et al., Identifying outdoor thermal risk areas and evaluation of future thermal comfort concerning shading orientation in a traditional settlement. Science of the Total Environment, 2018. 626: p. 567-580.
6. Perera, K., M. Donn, and M.A. Schnabel, Outdoor thermal comfort: A model based on thermal adaptation in New Zealand. 2020.
7. Tavares, S.G., S.R. Swaffield, and E.J. Stewart, A case-based methodology for investigating urban comfort through interpretive research and microclimate analysis in post-earthquake Christchurch, New Zealand. Environment and Planning B: Urban Analytics and City Science, 2019. 46(4): p. 731-750.
8. Tuller, S., Effects of a moderate sized city on human thermal bioclimate during clear winter nights. International journal of biometeorology, 1980. 24(1): p. 97-106.
9. De Freitas, C., et al., Microclimate and heat stress of runners in mass participation events. Journal of Applied Meteorology and Climatology, 1985. 24(2): p. 184-191.
10. Isaacs, N. and M.R. Donn, The Inclusion of Microclimate Modelling for House Heating Energy Simulation in Wellington, New Zealand. 2021.
11. Jalali, Z., et al., What we know and do not know about New Zealand's urban microclimate: A critical review. Energy and Buildings, 2022: p. 112430.
12. Tiatia, J., et al., Climate change, mental health and wellbeing: privileging Pacific peoples' perspectives–phase one. Climate and Development, 2022: p. 1-12.
13. Harrington, L.J., Rethinking extreme heat in a cool climate: a New Zealand case study. Environmental Research Letters, 2021. 16(3): p. 034030.
14. Mullan, B., et al., Climate change projections for New Zealand: atmosphere projections based on simulations from the IPCC fifth assessment. Wellington, Ministry for the Environment, 2016.
15. Paranunzio, R., et al., Assessing current and future heat risk in Dublin city, Ireland. Urban Climate, 2021. 40: p. 100983.
16. Hua, J., et al., Spatiotemporal assessment of extreme heat risk for high-density cities: A case study of Hong Kong from 2006 to 2016. Sustainable cities and society, 2021. 64: p. 102507.
17. Fowler, A.M., Using historical sources to supplement climate site histories: A case study of Auckland's Albert Park. New Zealand Geographer, 2020. 76(3): p. 225-236.
18. Blazejczyk, K., et al., Comparison of UTCI to selected thermal indices. International journal of biometeorology, 2012. 56: p. 515-535.
19. Shinzato, P., et al., Calibration process and parametrization of tropical plants using ENVI-met V4–Sao Paulo case study. Architectural Science Review, 2019. 62(2): p. 112-125.
20. Lachapelle, J.A., et al., A microscale three-dimensional model of urban outdoor thermal exposure (TUF-Pedestrian). International journal of biometeorology, 2022. 66(4): p. 833-848.
21. Chatzinikolaou, E., C. Chalkias, and E. Dimopoulou, URBAN MICROCLIMATE IMPROVEMENT USING ENVI-MET CLIMATE MODEL. International Archives of the Photogrammetry, Remote Sensing & Spatial Information Sciences, 2018.
22. Rui, L., et al. Study of the effect of green quantity and structure on thermal comfort and air quality in an urban-like residential district by ENVI-met modelling. in Building simulation. 2019. Springer.
23. Sara, L.M., et al., Risk perception: The social construction of spatial knowledge around climate change-related scenarios in Lima. Habitat International, 2016. 54: p. 136-149.
24. Lin, T.-P. and A. Matzarakis, Tourism climate and thermal comfort in Sun Moon Lake, Taiwan. International journal of biometeorology, 2008. 52: p. 281-290.
25. Fong, C.S., et al., Holistic recommendations for future outdoor thermal comfort assessment in tropical Southeast Asia: A critical appraisal. Sustainable Cities and Society, 2019. 46: p. 101428.
26. González, C.M.M., et al., Effects of future climate change on the preservation of artworks, thermal comfort and energy consumption in historic buildings. Applied energy, 2020. 276: p. 115483.

27. Zhang, S., et al., Physiological equivalent temperature-based and universal thermal climate index-based adaptive-rational outdoor thermal comfort models. Building and Environment, 2023. 228: p. 109900.
28. Ribeiro, K.F.A., et al., Calibration of the Physiological Equivalent Temperature (PET) index range for outside spaces in a tropical climate city. Urban Climate, 2022. 44: p. 101196.
29. Potchter, O., et al., Outdoor human thermal perception in various climates: A comprehensive review of approaches, methods and quantification. Science of the Total Environment, 2018. 631: p. 390-406.
30. Talbot, N., Air quality and societal impacts from predicted climate change in Auckland. 2019: Auckland Council, Te Kaunihera o Tāmaki Makaurau.
31. Nielsen, C.N. and J. Kolarik. Utilization of Climate Files Predicting Future Weather in Dynamic Building Performance Simulation–A review. in Journal of Physics: Conference Series. 2021. IOP Publishing.
32. Tahir, F., A.A. Baloch, and S.G. Al-Ghamdi, Impact of climate change on solar monofacial and bifacial Photovoltaics (PV) potential in Qatar. Energy Reports, 2022. 8: p. 518-522.
33. Shapiro, S.S. and M.B. Wilk, An analysis of variance test for normality (complete samples). Biometrika, 1965. 52(3/4): p. 591-611.
34. Hastie, T.J. and D. Pregibon, Generalized linear models, in Statistical models in S. 2017, Routledge. p. 195-247.
35. Allison, P., What's the best R-squared for logistic regression. Statistical Horizons, 2013. 13.
36. Armstrong, B.G. and M. Sloan, Ordinal regression models for epidemiologic data. American Journal of Epidemiology, 1989. 129(1): p. 191-204.
37. Christensen, R.H.B., Cumulative link models for ordinal regression with the R package ordinal. Submitted in J. Stat. Software, 2018. 35.
38. Jentsch, M., A. Bahaj, and P. James, CCWorldWeatherGen, Climate change world weather file generator, Version 1.8. Sustainable Energy Research Group, The University of Southampton, 2013.

Appendix A. Distribution of survey responses collected at both locations (n=347)

Variable	Value	Frequency	Relative Frequency	Percentage
Gender	Female	174	0.5014	50.14%
	Male	173	0.4986	49.86%
Age group	16-25	138	0.3977	39.77%
	26-40	149	0.4294	42.94%
	41-60	51	0.1470	14.70%
	Above 60	9	0.0259	2.59%
Activity	Light walk	38	0.1095	10.95%
	Sitting	170	0.4899	48.99%
	Standing	139	0.4006	40.06%
Clothing	One layer	269	0.7752	77.52%
	Two layers	63	0.1816	18.16%
	More than two layers	15	0.0432	4.32%
Thermal sensation	Neutral	128	0.3689	36.89%
	Slightly cool	9	0.0259	2.59%
	Slightly warm	157	0.4524	45.24%
	Warm	53	0.1527	15.27%
Humidity sensation	Neutral	317	0.9135	91.35%
	Dry	14	0.0403	4.03%
	Humid	16	0.0461	4.61%
Wind sensation	Neutral	171	0.4928	49.28%
	Windy	176	0.5072	50.72%
Thermal preference	No change	145	0.4179	41.79%
	Cooler	194	0.5591	55.91%
	Warmer	8	0.0231	2.31%

Period living in Auckland	Below one year	67	0.1931	19.31%
	1-5 years	114	0.3285	32.85%
	Above 5 years	166	0.4784	47.84%
Indoor air conditioning before survey	Yes	123	0.3544	35.44%
	No	224	0.6456	64.56%
Type of change preferred	Changing materials	20	0.0576	5.76%
	Increasing vegetation cover	291	0.8386	83.86%
	More shaded place	30	0.0865	8.65%
	More unshaded places	6	0.0173	1.73%
Nationality	New Zealand	132	0.3804	38.04%
	Others	215	0.6196	61.96%